Food and Bioprocess Technology (2020) 13:1462–1477
https://doi.org/10.1007/s11947-020-02479-w

ORIGINAL RESEARCH

Antimicrobial, Aflatoxin B_1 Inhibitory and Lipid Oxidation Suppressing Potential of Anethole-Based Chitosan Nanoemulsion as Novel Preservative for Protection of Stored Maize

Anand Kumar Chaudhari[1] · Vipin Kumar Singh[1] · Somenath Das[1] · Deepika[1] · Bijendra Kumar Singh[1] · Nawal Kishore Dubey[1]

Received: 27 February 2020 / Accepted: 10 June 2020 / Published online: 11 July 2020

Abstract

Aflatoxins (AFs) are the most frequent contaminants of maize and maize-based products, and its consumption can cause severe adverse effects to humans and animals. The efficacy of essential oils (EOs) and their bioactive compounds as potential antifungal agents has been well documented against food-borne fungi. This study evaluates the preservative potency of anethole-based chitosan nanoemulsion (Ant-eCsNe) to control deterioration of stored maize samples from fungal infestation, aflatoxin B_1 (AFB_1) contamination and lipid oxidation. Release study indicated a relatively good sustainable release profile for the encapsulated anethole after 10 days. The Ant-eCsNe showed improved efficacy against *A. flavus* (AF-LHP-VS8) and other common food-borne moulds and inhibited growth and AFB_1 biosynthesis at 0.8 and 0.4 μL/mL, respectively. Ant-eCsNe caused concentration-dependent inhibition of ergosterol content and increased efflux of cellular ions (Ca^{+2}, Mg^{+2} and K^+) and 260 and 280 nm absorbing materials, suggesting damage of fungal plasma membrane. Inhibition of methylglyoxal in fungal cells treated with Ant-eCsNe signifies its novel antiaflatoxigenic mechanism of action. Ant-eCsNe exhibited strong in vitro DPPH$^•$ and ABTS$^{+•}$ scavenging activity with IC_{50} value 89.36 and 45.05 μL/mL, respectively, and inhibited lipid oxidation in stored maize samples. Further, Ant-eCsNe exhibited reasonably strong efficacy in preserving maize samples from fungal and AFB_1 contamination during in vivo investigations and did not change the sensory attributes as well. Overall results revealed that Ant-eCsNe holds good potential to be applied as food preservative to reduce fungal and aflatoxin contamination causing deterioration of stored maize.

Keywords *Aspergillus flavus* · Encapsulation · Methylglyoxal · Food deterioration · In vitro release · Sensory profile

Introduction

Since their discovery in the late 1990s, aflatoxins (AFs) secreted by *Aspergillus flavus*, *A. parasiticus* and *A. nomius* in food items are among the most pervasive mycotoxin and emerged as the major risk factor responsible for severe health hazards to both human and animals (Rammanee and Hongpattarakere 2011; Gómez et al. 2018). Studies have shown that AFs are the most frequent mycotoxin contaminating several agricultural commodities, among which maize (*Zea mays* L.) is the most important cereal crop after wheat and rice, since it contributed a role in both food and feed supply throughout the world (Nishimwe et al. 2017), and hence, its contamination by AFs brings the rising concern among consumers regarding food safety. In addition, the lipid oxidation induced by oxidative stress is another major cause of food quality deterioration during storage resulting into unpleasant flavours, rancidity and loss of vital dietary constituents (Medeiros et al. 2014; Das et al. 2019). Different synthetic preservatives and antioxidants have been frequently applied to control the AFs contamination and lipid oxidation so as to extend the shelf-life of food commodities, but their indiscriminate use inevitably lead to unintended problems such as residual toxicity, environmental toxicity and the development of resistance (Contigiani et al. 2018). In recent pasts, the use of essential oils (EOs) and their bioactive components has been highly encouraged and attracted much attention as low-risk environmentally friendly and feasible alternatives to the most accepted but harmful synthetic preservatives. These multi-component bioactive EOs hold a broad range of

✉ Nawal Kishore Dubey
nkdubeybhu@gmail.com

[1] Laboratory of Herbal Pesticides, Centre of Advanced study (CAS) in Botany, Institute of Science, Banaras Hindu University, Varanasi 221005, India

antifungal, antiaflatoxigenic and antioxidant properties and in few cases also claim their efficacy in food system (Beyki et al. 2014; Chaudhari et al. 2019). However, their volatility, low bioavailability, oxidative instability and unfavourable effect on organoleptic characteristics may limit their application directly into food systems (Ezhilarasi et al. 2013; Guo et al. 2017). To address these challenges, encapsulation of bioactive compounds into nanomatrix using biological polymers is desirable (Ghaderi-Ghahfarokhi et al. 2016). Among different polymers used for the preparation of nanoemulsion, chitosan is perhaps the most studied and suitable encapsulating material owing to its abundance, biodegradability, GRAS status, high encapsulation efficiency, improved stability via acting as barrier against oxidation, mimicking undesirable effects and antimicrobial activities (Hasheminejad et al. 2019; Muxika et al. 2017). Indeed, it can also act as a reservoir and allow the desired compounds to reach the requisite concentration in the food without reaching the levels normal organoleptic acceptance.

Anethole (PubChem CID: 637563) is an aromatic compound found in EOs of plants, viz., *Syzygium anisatum*, *Foeniculum vulgare*, *Melissa officinalis* and *Coriandrum sativum* and used as a flavouring agent since antiquity (Kfoury et al. 2014). Due to nontoxic nature, it is also approved by the US-FDA as a safe flavouring and preservative agents of food items (Newberne et al. 1999). Recently, many reports on the antimicrobial and antioxidant activity of anethole have been published (Ye et al. 2017; Ksouda et al. 2019). However, none of the studies has been conducted to compare the antifungal, antiaflatoxigenic and antioxidant activity of un-encapsulated and encapsulated anethole against fungal, AFB_1 contamination and lipid oxidation as well as its in vivo efficacy in protection of stored maize samples.

The present study evaluated the potential of a single compound anethole present in EOs in contrast to essential oil as a whole. The main objective of the present study was to develop a controlled release system for anethole using chitosan as an encapsulant and tripolyphosphate as cross-linker and to assess their bioactivity and practical applicability. Hence, the study comprises synthesis of Ant-eCsNe, their characterization, assessment of antifungal, antiaflatoxigenic and antioxidant activity, mechanism of action, in vivo investigation on maize sample and sensory evaluation in comparison with that of un-encapsulated anethole to recommend their promising application in food system with consumer's acceptance.

Materials and Methods

Chemicals and Reagents

Chitosan (low molecular weight (LMW), degree of deacetylation > 90%), tripolyphosphate (TPP), dichloromethane (DCM), acetic acid, dimethyl sulfoxide (DMSO), methylglyoxal (MG), perchloric acid, Tween 20, Tween 80, methanol, DPPH and ABTS were procured from Hi-Media (Mumbai, India). Potato dextrose agar (PDA, composition included 100 g potato, 10 g dextrose, 7.5 g agar and 500 mL distilled water) and SMKY (composition included 100 g sucrose, 0.25 g $MgSO_4 \cdot 7H_2O$, 0.15 g KNO_3, 3.5 g yeast extract and 500 mL distilled water) were obtained from SRL (Mumbai, India). Anethole was kindly supplied by Ozone International (Mumbai, India).

Test Moulds

Aspergillus flavus strain (AF-LHP-VS8) along with nine other common food contaminating moulds, viz., *Aspergillus fumigatus*, *Aspergillus niger*, *Aspergillus luchuensis*, *Aspergillus repens*, *Penicillium italicum*, *Penicillium chrysogenum*, *Fusarium oxysporum*, *Alternaria alternata* and *Cladosporium cladosporioides*, were isolated from stored maize samples in our previous study (Chaudhari et al. 2018). The AF-LHP-VS8 (spore density = 1×10^6 spore/mL) culture was maintained as spore suspension.

Preparation of Anethole Encapsulated Chitosan Nanoemulsion (Ant-eCsNe)

Ant-eCsNe was fabricated through the ionic gelation technique using different ratio (w/v) of chitosan: anethole (1:0.2–1:1) with the dropwise addition of TPP as cross-linking agent. Chitosan is basically insoluble in its native form and hence required acidic environment with pH below 6.0 (therefore 1% acetic acid solution was used), which quaternizes the amine groups of chitosan and making them a soluble cationic electrolyte that effectively form the intra and intermolecular cross-linkages with the phosphate (anionic) backbone of TPP, resulting into the formation of stable nanoemulsion under constant stirring (Dash et al. 2011). The nanoemulsion was prepared following Hosseini et al. (2013) with few changes. Briefly, chitosan powder (1%, w/v) dispersed in distilled water holding 1% (v/v) anhydrous acetic acid solution was kept on magnetic stirrer (1000×*g*) for 12 h at 25 ± 2 °C. Tween 80 was then added as an emulsifier followed by an additional stirring for 2 h at 45 °C. The nanoemulsion was prepared by adding anethole admixed with DCM to the solution to reach final ratios (1:0.2, 1:0.4, 1:0.6, 1:0.8 and 1:1%) of chitosan to anethole (w/v), respectively, with homogenization (13,000×*g* for 10 min at 4 °C) using IKA, T18ED, homogenizer, Germany. A control solution (chitosan nanoemulsion (CsNe)) without anethole was also fabricated following the similar protocol. Consequently, the TPP solution (0.4 mg/mL) was added into chitosan solutions homogenized with anethole and to the solution devoid of anethole (CsNe) and stirred for 40 min followed by centrifugation (13,000×*g* for 10 min at 4 °C) using Remi Compufuse CPR-

4 (India). The obtained pellets were suspended in distilled water and subjected to ultrasonication (Sonics, Vibra Cell) for 8 min. Finally, the nanoemulsions were placed in round bottom flasks and lyophilized using freeze dryer (Alpha 1–2 LD plus model, Sydney, Australia). Prior to lyophilization, the nanoemulsions were held at − 20 °C in a deep freezer for 24 h. The flasks were then sealed with the valves of lyophilization caps and frozen at ultralow temperature (− 80 °C) for 30 min. After that, main drying phase was carried out for 3 days at − 52 °C and at a pressure of 0.1 amber. After completion of lyophilization, the samples were sealed in a screw capped vials and stored under − 20 °C prior to further characterization.

Nanoentrapment Efficiency (NE%) and Loading Capacity (LC%) Determination

The total amount of anethole entrapped into CsNe was assessed using UV-visible spectrophotometer (UV-2600, Shimadzu, Japan) at 244 nm. In brief, a total of 100 μL Ant-eCsNe were mixed with 3 mL hexane, swirled and centrifuged at 13,000×*g* for 10 min. CsNe was considered as blank. The obtained supernatants were used to record the absorbance at 244 nm, and the total amount of anethole encapsulated into Ant-eCsNe was calculated from the Eq. ($Y = 0.078x - 0.005$; $R^2 = 0.998$) obtained using different amount of pure anethole into hexane. The experiment was repeated thrice and NE and LC percentage were calculated according to the following equations:

$$\text{Per cent NE} = \frac{\text{Total mass of anethole entrapped into nanoemulsion}}{\text{Initial mass of anethole added into chitosan solution}} \times 100$$

$$\text{Per cent LC} = \frac{\text{Total mass of anethole entrapped into nanoemulsion}}{\text{Mass of nanoemulsion after lyophilization}} \times 100$$

Characterization of Nanoemulsion

Fourier-Transform Infrared (FTIR) Spectroscopic Analysis

FTIR analyses were conducted for chitosan, CsNe, anethole and Ant-eCsNe in KBr disk using FTIR spectroscopy (Perkin Elmer). The spectra were obtained in the range of 500 to 4000 cm^{-1} with a resolution of 4 cm^{-1}.

Scanning Electron Microscopy (SEM) Analysis

The surface morphology of CsNe and Ant-eCsNe was examined using a SEM (EVO 18 Research, Zeiss, Germany). For this purpose, briefly 5 mg lyophilized powder of CsNe and Ant-eCsNe was dissolved in 20 mL of distilled water, sonicated and a drop of it was placed on a cover glass followed by air drying at room temperature. The films were then allowed to sputtering with gold in a sputter (DSR 1 coater). The representative SEM images were reported at different magnifications.

X-Ray Diffraction (XRD) Analysis

The XRD patterns demonstrating the crystallographic profiles of chitosan, CsNe and Ant-eCsNe were achieved using a Bruker D8 diffractometer operated at 40 kV. Radial scan intensity was recorded over the range of 2θ angle = 5–50° with a scanning of 1° min^{-1} and step angle 0.02° min^{-1} at room temperature.

Kinetics of In Vitro Release Profiles of Ant-eCsNe

The release study of anethole was carried out in phosphate buffer saline (PBS) following Hosseini et al. (2013) with slight modifications. Firstly, Ant-eCsNe (1 mL) was added to glass vial containing 10 mL of PBS (pH 7.4) and kept at room temperature for 10 days. An aliquot of 1 mL was withdrawn at specific time intervals and replenished with the same amount of buffer to maintain the constancy. The concentration of anethole was measured at the absorbance of 274 nm using the UV-visible spectrophotometer. The amount of anethole released in the medium was calculated from the calibration curve of pure anethole obtained in PBS solution using following equation:

$$\text{Invitro release (\%)} = \frac{\text{Amount of released anethole at each sampling day}}{\text{Initial amount of anethole encapsulated in the sample}} \times 100$$

Antifungal and Antiaflatoxigenic Evaluation of Anethole and Ant-eCsNe

The efficacy of anethole and Ant-eCsNe on growth of test fungus (AF-LHP-VS8) and nine other food contaminating moulds (*A. fumigatus*, *A. niger*, *A. luchuensis*, *A. repens*, *P. italicum*, *P. chrysogenum*, *F. oxysporum*, *A. alternata* and *C. cladosporioides*) was evaluated in terms of minimum inhibitory concentration (MIC) and fungitoxic spectrum, respectively, following the modified method of Dwivedy et al. (2018). For MIC, briefly, different doses of anethole (previously diluted in tween 20) and Ant-eCsNe was individually added to conical flask containing SMKY medium to obtain the final concentrations of 0.2, 0.4, 0.6, 0.8, 1.0 and 1.2 μL/mL. In each medium, 25 μL of AF-LHP-VS8 spore suspension (1×10^6 spore/mL) was inoculated and incubated at 25 ± 2 °C for 10 days. As controls, the flasks were supplemented with the same amount of tween 20 and CsNe instead of anethole and Ant-eCsNe, respectively. The fungitoxic spectrum of anethole and Ant-eCsNe was determined in Petri plates containing PDA medium at MIC (1.2 and 0.8 μL/mL, respectively) doses by inoculating a 5-mm fungal disk of each food-contaminating mould onto the centre of each plates.

Controls were prepared in the same ways as in MIC. After 7 days of incubation at 25 ± 2 °C, the developed colony diameter was measured, and the per cent fungal inhibition (FI) was calculated following formula:

$$\%\mathrm{FI} = \frac{\text{Colony diameter in control–Colony diameter in treatment}}{\text{Colony diameter in control}} \times 100$$

To determine the antiaflatoxigenic activity, the contents of each flask were filtered, and the mycelial content left were placed in oven for the determination of mycelial dry weight, while the filtrates were agitated in a separating funnel with 20 mL of chloroform. Next, chloroform fraction were vaporized on hot water bath until dryness, and the residues were dissolved with 1 mL of methanol, and 50 μL of it was loaded on silica gel plate followed by toxin separation in mobile phase (toluene (45): isoamyl-alcohol (16): methanol: (1), v/v/v) system. Thereafter, the plates were air-dried, visualized under transilluminator, and the appeared spots were re-suspended in 5 mL cold methanol. After centrifugation for 5 min at 3000×*g*, the absorbance of the supernatant was recorded at 360 nm, and the amount of AFB_1 in the sample was calculated by the given equation:

$$\mathrm{AFB_1\ content\ (\mu g/mL)} = \frac{D \times M}{E \times L} \times 1000 \times 1000$$

where *D* is the absorbance, *M* is the molecular mass of AFB_1 (312 g/mol), *E* is the molar extinction coefficient (21, 800/mol cm^{-1}) and *L* is path length (1 cm).

Further, the inhibition percentage of AFB_1 was calculated as follows:

$$\mathrm{Inhibition\ (\%)} = \frac{Y - X}{Y} \times 100$$

where *Y* is the mean AFB_1 concentration in the control and *X* is the mean AFB_1 concentration in the treatments.

Antifungal Mechanism of Action of Anethole and Ant-eCsNe

The antifungal mechanism of action was investigated in terms of ergosterol inhibition and efflux of cellular ions (Ca^{+2}, Mg^{+2} and K^+) and 260 and 280 nm absorbing materials. To quantify ergosterol, briefly, the spore suspension (25 μL) of AF-LHP-VS8 was aseptically inoculated in medium (SMKY) bearing 0.2, 0.4, 0.6, 0.8, 1.0 and 1.2 μL/mL of anethole and Ant-eCsNe. Samples without anethole and Ant-eCsNe were served as controls. After 4 days of incubation at 25 ± 2 °C, the developed mycelia were autoclaved, washed and fresh weight were measured. Subsequently, the mycelia were transferred into culture tube containing 5 mL of alcoholic KOH (25%) solution, vortexed (3 min) and kept on hot water bath for 2 h. After cooling at room temperature, the ergosterol present in the sample was extracted by adding 2 mL of extra pure water and 5 mL n-heptane, followed by shaking for 3 min. Prior to analysis, the upper transparent layer was collected and scanned using UV-visible spectrophotometer within the range of 230 to 300 nm. Ergosterol was calculated using the following equations

$$\%\,\text{ergosterol} + \%24\,(28)\,\text{dehydroergosterol} = (A_{282}/290)/\text{pellet weight}$$

$$\%\,24\,(28)\,\text{dehydrosterol} = (A_{230}/518)/\text{pellet weight}$$

$$\%\,\text{ergosterol} = (\%\text{ergosterol} + \%24(28)\,\text{dehydroergosterol}) - \%24(28)\,\text{dehydroergosterol}.$$

where *290* and *518* are the *E* values determined for crystalline ergosterol and dehydroergosterol, respectively.

The efflux of Ca^{+2}, Mg^{+2} and K^+ ion was measured according to the method of Das et al. (2019) with some modifications. Firstly, 50 μL spore suspension of AF-LHP-VS8 was grown in SMKY medium and incubated for 4 days at 25 ± 2 °C. The developed mycelia were collected, washed and added in culture tube containing 20 mL of saline solution bearing anethole and Ant-eCsNe at three different concentrations, i.e. 1/2MIC, MIC and 2MIC. After overnight incubation, the contents were filtered, and the filtrates were analysed for cellular ions using atomic absorption spectroscopy (Aanalyst 800, Perkin Elmer, USA). For the measurement of 260 and 280 nm absorbing materials, a 4-day old culture of AF-LHP-VS8 was collected, washed and added to culture tube containing 20 mL of PBS solution bearing anethole and Ant-eCsNe at 1/2MIC, MIC and 2MIC doses. After overnight incubation at 25 ± 2 °C, the samples were collected, centrifuged (13,000×*g* for 10 min) and subjected to absorbance measurement at 260 and 280 nm.

Antiaflatoxigenic Mechanism of Action of Anethole and Ant-eCsNe

The mechanism of AFB_1 suppression was investigated by measuring the level of methylglyoxal (MG) (substrate inducing aflatoxin biosynthesis) in the fungal cells treated with different concentrations of anethole and Ant-eCsNe following Upadhyay et al. (2018). Briefly, 0.3 g biomass of AF-LHP-VS8 previously grown in SMKY medium was treated with desired concentrations (0.2, 0.4, 0.6, 0.8, 1.0 and 1.2 μL/mL) of anethole and Ant-eCsNe. The controls without anethole and Ant-eCsNe were also prepared for the following measurement. After overnight incubation, the fungal biomass was crushed in 3 mL (0.5 M) perchloric acid and placed on ice bath for 10 min followed by centrifugation at 13000×*g* for 10 min. The filtrate obtained was then adjusted to neutral pH (7.0) by adding potassium carbonate solution and centrifuged again. To perform MG assay, in a total of 2 mL, 500 μL of 7.2 mM 1,2-diaminobenzene (DAB), 200 μL of 5 M perchloric acid and 1.3 mL of sample obtained after centrifugation were

added in the same order. The absorbance of the sample was recorded at 341 nm using UV-visible spectrophotometer, and the total MG was calculated using standard equation prepared using 10–100 μM of pure MG.

In Vivo Antifungal and Antiaflatoxigenic Evaluation of Anethole and Ant-eCsNe

The maize sample (Varun Suma) was selected as a model food system to perform the in vivo antifungal and antiaflatoxigenic efficacy of anethole and Ant-eCsNe. Maize is one of the most important cereal crop of the world, and its contamination by AFB_1 is of great concern, since this agricultural crop plays a major role in both food and feed supply worldwide (Battilani et al. 2016). Moreover, the presence of high starch content in maize kernel and favourable environmental conditions during storage make them susceptible towards *A. flavus* and subsequently with AFB_1 contamination (a potent human hepatocarcinogen), which bring the rising concerns regarding food security (Kos et al. 2013; Mahuku et al. 2019). Based on these facts, herein, maize samples were chosen as model food system to investigate the preservative efficacy of anethole and Ant-eCsNe. In view of results obtained during in vitro evaluation, an artificial inoculation of this sample was conducted with test fungus (AF-LHP-VS8). Prior to antifungal evaluation, the sample (200 g) was surface sterilized with 0.1% sodium hypochlorite solution and divided into three groups in Petri plates, viz., inoculated controls (maize sample inoculated with 100 μL spore suspension), inoculated treatment at MIC (maize sample inoculated with 100 μL spore suspension and treated with anethole and Ant-eCsNe at 1.2 and 0.8 μL/mL, respectively) and the inoculated treatment at 2MIC (sample inoculated with 100 μL spore suspension and treated with anethole and Ant-eCsNe at 2.4 and 1.6 μL/mL, respectively). All sets were kept under 25 ± 2 °C (temperature suitable for fungal growth) in BOD for 2 weeks, and the visual observation of fungal growth was performed. To determine the extent of AFB_1 inhibition, briefly 10 g of well-milled maize samples from aforementioned experiments were weighed to 1 mg and mixed with methanol: water (8:10, v/v) by shaking on mechanical shaker (30 min) followed by centrifugation at 5000×g for 5 min. The obtained supernatant was then separated in conical flasks and mixed with 300 μL of chloroform and 6 mL Millipore water bearing 3% KBr. After an additional centrifugation at 5000×*g* for 5 min, the settled phase was separated in a centrifuge tube and evaporated on hot water bath until dryness. The obtained residues were dissolved with 100 μL of methanol (HPLC grade) and injected to HPLC system coupled with C-18 reverse phase column. The sample was separated at a flow of 1.2 mL/min in a mobile phase solvent system consisting of a mixture (17:90:64, v/v/v) of methanol: acetonitrile and Millipore water. The AFB_1 was quantified at an excitation wavelength of 360 nm.

Antioxidant Activity of Anethole and Ant-eCsNe

The antioxidant capacity of anethole and Ant-eCsNe was determined in terms of radical scavenging activity using the stable free radicals, i.e. $DPPH^{\bullet}$ and $ABTS^{+\bullet}$ following the procedure described elsewhere (Avanço et al. 2017). For DPPH assay, briefly, different concentrations (20–200 μL/mL) of anethole and Ant-eCsNe (dissolved in DMSO) were added to the $DPPH^{\bullet}$ solution (2 mL) prepared in methanol. The decrease in absorbance was recorded after 30 min at 517 nm against corresponding blank using UV-visible spectrophotometer. The ABTS assay was performed in two steps: firstly, $ABTS^{+\bullet}$ radical was formed by reacting 7 mM pure ABTS with 2.54 mM potassium per sulphate, and the resulting mixture was kept under dark condition for overnight. The mixture was diluted with ethanol to achieve the absorbance 0.70 ± 0.05 at 734 nm. Then, different concentrations (8–80 μL/mL) of anethole and Ant-eCsNe were allowed to react with $ABTS^{+\bullet}$ solution (2 mL), and after 6 min of reaction, the absorbance was recorded at 734 nm. The antioxidant capacity was evaluated by plotting the concentrations of anethole and Ant-eCsNe against the per cent radical scavenging activity, and inhibition was calculated from the following formula:

$$\text{Per cent radical scavenging capacity} = (A_0 – A_1)/A_0 \times 100$$

where A_0 and A_1 are the absorbance of blank as well as sample at 515 and 734 nm for DPPH and ABTS, respectively.

Effect of Anethole and Ant-CsNe on Inhibition of Lipid Oxidation

The extent of lipid oxidation inhibition in maize sample treated with anethole and Ant-CsNe at their respective MIC and 2MIC was determined in terms of malondialdehyde (MDA) content through thiobarbituric acid reactive substance (TBARS) according to the modified method of Fan (2002). Briefly, 1 g milled maize sample from treated as well as control (without anethole and Ant-CsNe) sets were added to thiobarbituric acid (TBA) reagent consisting of 0.375% TBA dissolved in 15% trichloroacetic acid (TCA) and 0.2 N HCl. The mixtures were heated on water bath at 90 °C for 30 min, cooled and then centrifuged at 13,0000×g for 10 min. Finally, the absorbance of the supernatant was recorded at 532 and 600 nm. The results were expressed as μM equivalent MDA/g FW.

Sensory Analysis: Effect on Organoleptic Attributes

The application of single compound with better antimicrobial potential in food application is more preferable as this would

minimally alter the sensory profile of food system. To assess the effect of aromatic profile of anethole before and after encapsulation into chitosan nanoemulsion, a sensory test was conducted on maize samples treated with anethole and Ant-eCsNe at their respective MIC doses after 2 weeks of storage at room temperature using a seven-point hedonic scale (7 = extremely good, 6 = moderately good, 5 = slightly good, 4 = neither good nor bad, 3 = moderately bad, 2 = slightly bad and 1 = extremely bad). Samples without treatments were considered as control. Prior to analysis, the samples were roasted in an oven and served to a group of 10 semi-trained individuals of both genders (age between 25 and 48 years) and asked to assess the colour, texture, flavour, mouth feel and overall acceptability of the samples. Before beginning the roasting process, the oven was preheated for 30 min to ensure that the steady-state was reached. Then, approximately 100 g of the maize samples were placed in an oven and roasted for a minute by stimulating the commercial roasting temperature condition (100 °C). The samples were then removed from the oven and allowed to cool at room temperature and served to the assessors for sensory analysis.

Statistical Analysis

All the experiments were carried out thrice and the results were expressed as mean ± standard error (SE). The statistical significance was compared between control and treatments by one-way analysis of variance (ANOVA) followed by Tukey's B multiple comparisons test using software SPSS (version 16.0, Chicago, IL, USA). The 0.05 level of probability was taken as the minimum level of significance.

Results and Discussion

Preparation of Anethole-Enriched Chitosan Nanoemulsion (Ant-eCsNe)

The nanoencapsulation performed in the present study has advantages over the free bioactive compounds, since it enhances the stability and overcomes the drawbacks related to their large-scale employment as efficient natural preservatives. Moreover, the selection of chitosan as encapsulating agent to encapsulate the anethole is another advantage as it is easily available in nature, showing high encapsulation efficiency towards lipophilic bioactive compounds, promising antifungal activity and compatibility with the food bioactive constituents (Othman et al. 2018). Ionic gelation is a novel and one of the simplest techniques to fabricate chitosan-enriched nanoemulsion reported so far in the literature. The success of this technique over other conventional methods mainly relies on its single-shot synthesis, low cost and requirement of mild environmental conditions for the synthesis of reproducible, monodisperse, stable and nanorange-sized chitosan nanoemulsion (Bugnicourt and Ladavière 2016). In fact, the fabrication of chitosan nanoemulsion in aqueous medium via ionic gelation is particularly adequate to encapsulate hydrophobic compounds like anethole to make them easily transformable for industrial scale use as a promising food preservative. On the other hand, the antimicrobial nature and non-toxic profile of both anethole and chitosan along with their biocompatibility with food bioactive components are particularly interesting for application in food industries in comparison with other synthetic antimicrobials such as quaternary ammonium salts and propionic, benzoic and sorbic acids (Carocho et al. 2014). By using this approach, Hosseini et al. (2013) successfully encapsulated oregano essential oil in chitosan nanoparticle and reported that the ionic gelation can enhance the encapsulation efficiency, antimicrobial activity and stability and achieve controlled release, hence facilitating the development of natural bioactive compound-based chitosan nanoemulsion over synthetic preservatives for application in the food industries.

Per Cent NE and LC Determination

Table 1 shows the per cent of NE and LC of anethole into Ant-eCsNe. The results obtained through UV-visible spectrophotometric analysis revealed that NE increased from 19.9 to 76.1% when the chitosan to anethole ratio ranged from 1:0.2 to 1:0.8 and then dropped off to 40.8% when ratio of anethole further increased; however, the LC increased as a function of initial anethole content with the values ranging from 0.3 to 5.9%. This trend of NE was found in good agreement with the earlier study of Keawchaoon and Yoksan (2011) and Pabast et al. (2018), who reported good encapsulation efficiency at optimal ratio, during measuring the encapsulation efficiency of carvacrol into chitosan-TPP nanoparticles and cholesterol impregnated into lecithin nanoliposome, respectively. This declining trend of NE could be ascribed to the insufficiency of chitosan required for additional entrapment of test compound. Due to this fact and considering the high NE, nanoemulsion synthesized using the initial anethole content of 0.8% with respect to the chitosan (1%) was selected for the rest of the investigations. Further, the findings signify that a very small amount of anethole was lost during nanoemulsion preparation, and most of them were encapsulated. The NE and LC of anethole into Ant-eCsNe were found far better and satisfactory than some of the previously reported food preservatives such as EOs (oregano, thyme and cumin EO) (Hosseini et al. 2013; Lin et al. 2018; Amiri et al. 2020), bioactive compounds (gallic acid and thymol) (Aydogdu et al. 2019; Robledo et al. 2018) and synthetic one like quaternary ammonium salts (Wei et al. 2019), demonstrating the suitability of using anethole-based chitosan nanoemulsion in food industry.

Table 1 Nanoentrapment efficiency (NE%) and loading capacity (LC%) of Ant-eCsNe produced with different chitosan: anethole ratio

Chitosan: anethole (w/v)	NE%	LC%
1.0: 0.0	0.0 ± 0.0[a]	0.0 ± 0.0[a]
1.0: 0.2	19.9 ± 1.1[b]	0.3 ± 0.0[a]
1.0: 0.4	28.4 ± 1.2[c]	0.8 ± 0.0[a]
1.0: 0.6	41.6 ± 2.7[d]	2.0 ± 0.2[b]
1.0: 0.8	76.1 ± 1.0[e]	4.9 ± 0.1[c]
1.0: 1.0	40.8 ± 1.4[d]	5.9 ± 0.4[d]

Values are presented as mean ± SE ($n = 3$)

[a–e] Significant differences at $p < 0.05$ level according to ANOVA (Tukey's B) multiple comparisons test

Characterization of Nanoemulsion

FTIR Analysis

FTIR analyses were performed to explore the structural and chemical interaction between the chitosan and the test compound anethole incorporated in it. Figure 1 a–d showed the FTIR spectra obtained for chitosan, CsNe, anethole and Ant-eCsNe. The FTIR spectrum of chitosan displayed characteristic absorption bands at 3426 cm^{-1} for –OH and –NH stretching vibration, 2939 cm^{-1} for –CH stretching vibration, 1642 cm^{-1} for amide I, 1380 cm^{-1} for $–CH_3$ stretching and 1099 cm^{-1} for C–O–C bridge stretching. It could be noted that in CsNe, the peak at 1642 cm^{-1} of chitosan is shifted to 1655 cm^{-1} and two new absorption peaks, one at 1543 cm^{-1} for amide-II and second at 897 cm^{-1} for P–O–C stretching, appeared, indicating involvement of electrostatic interaction between chitosan and TPP (Yoksan et al. 2010). Pure anethole showed sharp peaks at 2985 cm^{-1} for aromatic –CH stretching vibration, 1727 cm^{-1} for ether group, 1600–1445 cm^{-1} corresponding to phenyl ring, 1297 cm^{-1} for –OH bending, and 1073 cm^{-1} and 746 cm^{-1} for C–C vibrations. The major spectra corresponding to CsNe and anethole also appeared in Ant-eCsNe. This was presumably due to inclusion of anethole into CsNe. Such characteristic changes in spectral peaks of chitosan nanoemulsion after addition of anethole and cross-linking TPP molecule confirmed the successful encapsulation of anethole into stable chitosan nanoemulsion advocating employment in food industries. Hosseini et al. (2013) also used FTIR to investigate the inclusion complex formation of oregano EO (OEO) and chitosan and showed that all the absorption peaks of chitosan, chitosan nanoparticle and OEO reappeared in OEO-loaded chitosan nanoparticle, confirming incorporation of OEO into the chitosan.

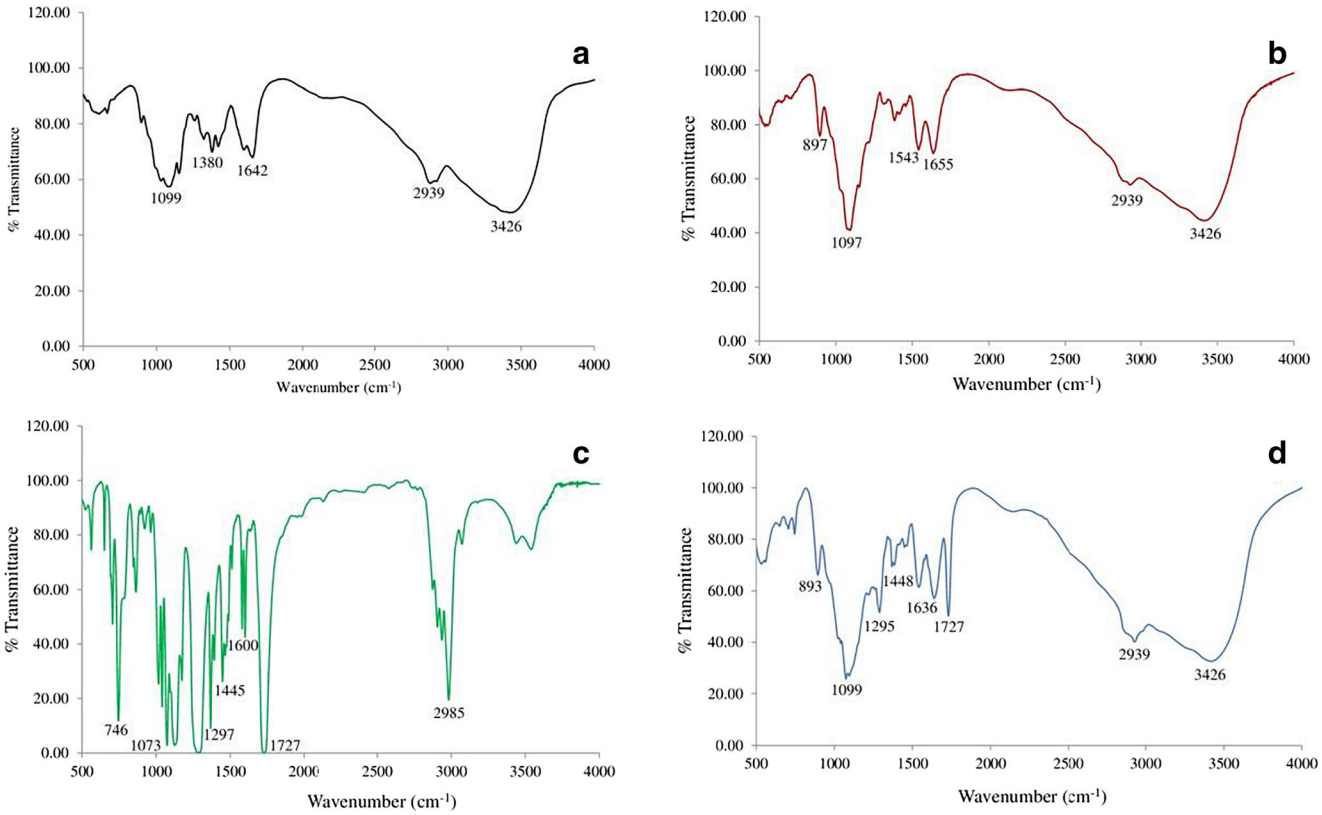

Fig. 1 FTIR spectra of (**a**) chitosan, (**b**) CsNe, (**c**) anethole and (**d**) Ant-eCsNe

SEM Analysis

The morphology of fabricated CsNe and Ant-eCsNe was determined using SEM, and respective images are presented in Fig. 2 a and b. Spherical shapes with nanometre-sized particles were observed for both CsNe and Ant-eCsNe. As it can be seen, CsNe had an average size ranging from 28.99 to 49.88 nm. However, when anethole was added into the chitosan nanoemulsion, the size was increased to 32.69–59.92 nm. This increase in size may be related to the successful encapsulation of anethole into CsNe. The increased size of capsules in nanoemulsion after encapsulation has been also reported by earlier authors (Keawchaoon and Yoksan 2011; López-Meneses et al. 2018); however, the size may vary depending on experimental methods and conditions. Considering the obtained results, it can be concluded that the formed nanoemulsion prepared using 1:0.8 (w/v) ratio of chitosan to anethole appeared to be very small in size (approximately < 100 nm) and might exhibited two significant properties including (a) improved physico-chemical properties and stability and (b) increased surface-to-volume ratio, which facilitates their reactivity, biological activities and controlled release profile, hence optimizing the amounts of anethole required for nanoemulsion preparation and use in food industries as a compatible nanoemulsion over harmful synthetic preservatives to extend the shelf-life of stored food commodities (Gahruie et al. 2017; Prakash et al. 2018).

XRD Analysis

Figure 2 c shows the crystallographic profiles of chitosan, CsNe and Ant-eCsNe analysed by XRD analysis. The diffractogram of pure chitosan showing two shoulder peaks with intensity maxima (2θ) of around 10.9° and 20° assigned the existence of amorphousness and high degree of crystallinity in chitosan (Osorio-Madrazo et al. 2010). On the other hand, CsNe and Ant-eCsNe showed reduction in peak heights with more broadening, which means that the crystallinity of chitosan was decreased after the addition of TPP and anethole. This might be due to modifications in the arrangement pattern of molecules in crystal lattice structure of chitosan. The crystallinity of chitosan can describe its useful application, since

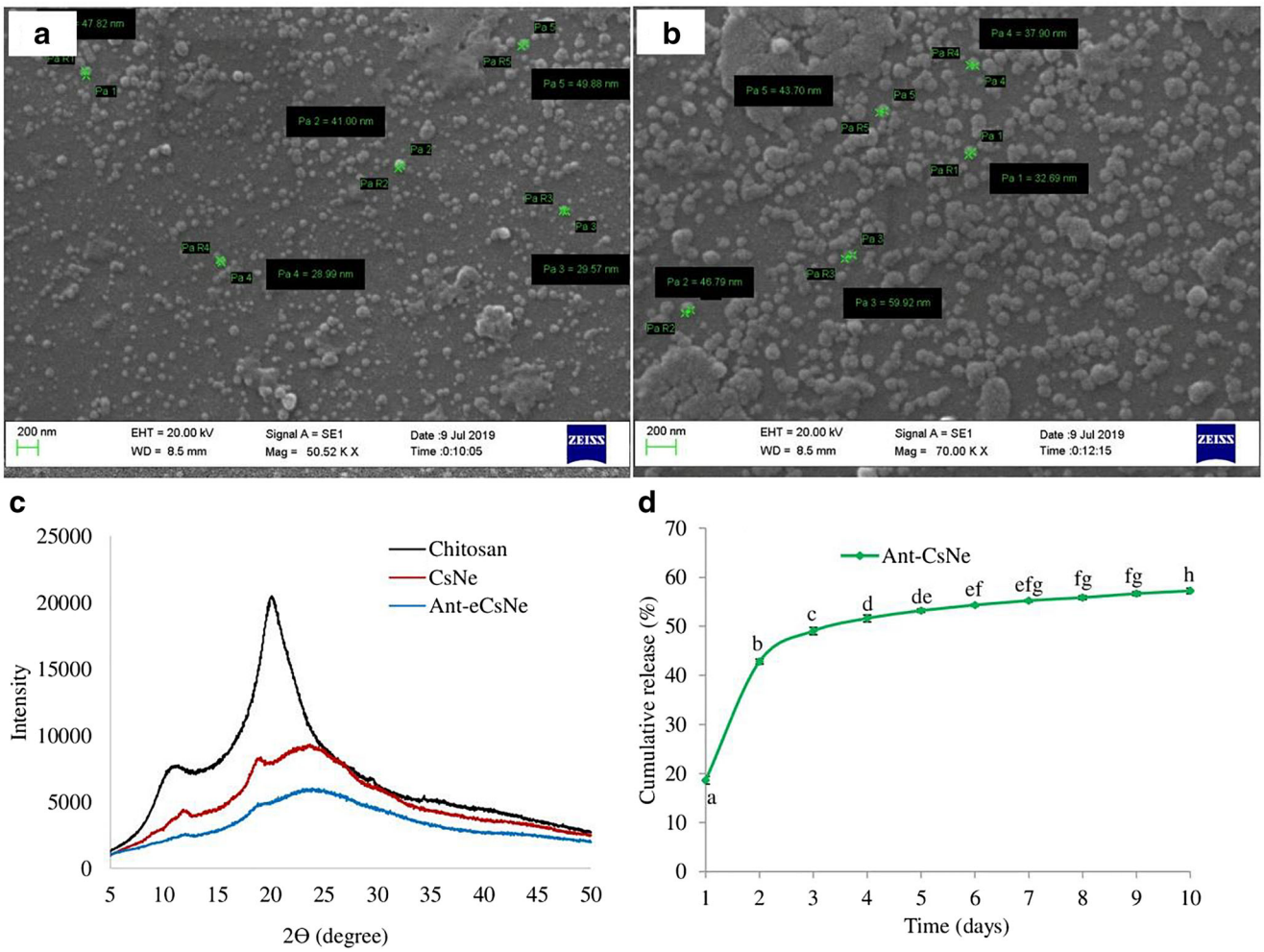

Fig. 2 **a** and **b** SEM micrographs of CsNe and Ant-eCsNe. **c** XRD patterns of chitosan, CsNe and Ant-eCsNe. **d** In vitro release profiles of Ant-eCsNe

the greater the crystallinity is the greater the stability due to tight packaging of molecules in chitosan (Lim et al. 2008). The absence of peak in chitosan nanoemulsion after the addition of 0.8% anethole reflected the destruction of their native packaging structure, suggesting encapsulation of anethole in its active form and compatibility for application in food system.

Kinetics of In Vitro Release Profiles of Ant-eCsNe

The in vitro release profiles of anethole from Ant-eCsNe at different time intervals are shown in Fig. 2 d. The release occurred in biphasic ways, i.e. initial burst release (42.8%) of anethole was recognized for the first 2 days of assay followed by constant release in the next 9 days. Maximum release observed was 57.2%, indicating that 18.8% of the anethole out of 76.1% was still entrapped within Ant-eCsNe. The initial burst release followed by controlled release might be related to the leaching of anethole which was not properly entrapped within the core of chitosan matrix or due to the phenomenon of diffusion, where the anethole moves from the high concentration to low concentration and continues until the concentration equilibrium is reached. The initial burst release was attributed to the anethole adsorbed on the surface of chitosan nanoemulsion and entrapped near the surface; since dissolution rate of chitosan close to the surface is high, the quantity of release will be also high (Anitha et al. 2011). Moreover, the pH of the medium plays an important role in initial burst release of anethole and other bioactive compounds. The release of encapsulated compounds is influenced by changes in pH. Studies have shown faster release in acidic medium than in basic or neutral, since at lower pH, the nanoemulsion matrix swells due to protonation of amine groups of chitosan polymer resulting into structural changes, thereby facilitating faster anethole release (Jayakumar et al. 2007). This kind of release behaviour has also been observed by Ahmadi et al. (2018) and Das et al. (2019) while demonstrating the in vitro release of *Satureja hortensis* and *Coriandrum sativum* EO loaded into chitosan nanoparticles, respectively. Thus, sustained release of anethole in subsequent days of assay affirmed the stability of Ant-eCsNe and proving its safe, convenient and efficacious effect on preservative potential for long-term industrial utilization for shelf-life extension of stored food items.

Antifungal and Antiaflatoxigenic Evaluation of Anethole and Ant-eCsNe

Results for antifungal and antiaflatoxigenic activity of anethole and Ant-eCsNe against AF-LHP-VS8 at tested concentrations are presented in Table 2. Anethole completely inhibited the visible growth and AFB_1 biosynthesis at 1.2 and 0.8 μL/mL, respectively. Surprisingly, as we expected, Ant-eCsNe was found more efficacious than the anethole where complete inhibition of growth and AFB_1 synthesis was being observed at 0.8 and 0.4 μL/mL, respectively. In addition, anethole at 1.2 μL/mL (MIC) inhibited the growth of six (*A. niger*, *A. luchuensis*, *P. chrysogenum*, *F. oxysporum*, *A. alternata* and *C. cladosporioides*) out of nine (*A. fumigatus*, *A. niger*, *A. luchuensis*, *A. repens*, *P. italicum*, *P. chrysogenum*, *F. oxysporum*, *A. alternata* and *C. cladosporioides*) tested moulds; however, the Ant-eCsNe at 0.8 μL/mL (MIC) concentration displayed broad-spectrum toxicity over un-encapsulated anethole and completely checked the growth of all tested moulds (Table 3). The results are in agreement with those obtained by Beyki et al. (2014) and Dwivedy et al. (2018) showing the enhanced performance of *Mentha piperita* and *Illicium verum* EO, respectively, after encapsulation into chitosan against *A. flavus* and other common moulds causing deterioration of stored food samples. Moreover, the MIC of Ant-eCsNe was found much greater than some of the previously reported synthetic antifungal preservatives, viz., ceresan, ziram, bavistin, nystatin and Wettasul-80 (Kumar et al. 2008; Prakash et al. 2010), strengthening its practical utilization as a potential antifungal agent. The enhanced antifungal efficacy of anethole after nanoencapsulation was possibly attributed to the synergism between the antifungal activity of anethole and chitosan itself or due to increased dispersion of anethole into aqueous environment and stimulation of passive adsorption mechanism into fungal cells (Donsì et al. 2011). Moreover, enhanced antiaflatoxigenic activity of Ant-eCsNe at lower concentration may be due to adsorptive property of chitosan with AFB_1 via preferred interaction established between the cationic charges of chitosan with the anionic charges of oxygenated lactone ring of AFB_1 (Juárez-Morales et al. 2017). Thus, using anethole within chitosan nanoemulsion (having enhanced efficacy) instead of anethole alone could be an attractive strategy for more efficient preservation of stored food commodities over most widely accepted but harmful synthetic preservatives against fungal and AFB_1 contamination.

Antifungal Mechanism of Action of Anethole and Ant-eCsNe

In the present investigation, a concentration-dependent inhibition of ergosterol content with increasing the concentrations of anethole and Ant-eCsNe was observed (Fig. 3a and b). The ergosterol content was decreased by 15.7, 43.7, 54.4, 82.3 and 100%, respectively, when AF-LHP-VS8 was treated with 0.2, 0.4, 0.6, 0.8 and 1.0 μL/mL concentrations of anethole, while for Ant-eCsNe the inhibition was 41.3, 83.1 and 100% at 0.2, 0.4 and 0.6 μL/mL, respectively. Interestingly, the ergosterol reduction was 100% at the concentration lower than the MIC values of both anethole and Ant-eCsNe in the similar ways as has been observed for AFB_1 inhibition. This finding signifies that there may be a positive relationship between ergosterol

Table 2 Effect of different concentrations of anethole and Ant-eCsNe on mycelial biomass and aflatoxin B_1 (AFB_1) production

Conc. (μL/mL)	Anethole		Ant-eCsNe	
	Mycelial biomass (g)	AFB_1 (μg/mL)	Mycelial biomass (g)	AFB_1 (μg/mL)
Control	0.38 ± 0.01[a]	2.39 ± 0.04[a]	0.36 ± 0.01[a]	2.38 ± 0.04[a]
0.2	0.35 ± 0.02[a]	1.96 ± 0.05[b]	0.26 ± 0.01[b]	0.80 ± 0.12[b]
0.4	0.27 ± 0.02[b]	1.45 ± 0.07[c]	0.13 ± 0.01[c]	0.00 ± 0.00[c]
0.6	0.17 ± 0.01[c]	0.80 ± 0.10[d]	0.06 ± 0.02[d]	0.00 ± 0.00[c]
0.8	0.14 ± 0.01[c]	0.00 ± 0.00[e]	0.00 ± 0.00[e]	0.00 ± 0.00[c]
1.0	0.06 ± 0.03[d]	0.00 ± 0.00[f]	0.00 ± 0.00[e]	0.00 ± 0.00[c]
1.2	0.00 ± 0.00[d]	0.00 ± 0.00[f]	0.00 ± 0.00[e]	0.00 ± 0.00[c]

Values are presented as mean ± SE ($n = 3$)

[a–f] Significant differences at $p < 0.05$ level according to ANOVA (Tukey's B) multiple comparisons test

and AFB_1 biosynthesis supporting the earlier investigation of Castro et al. (2002). Similarly, the efflux of Ca^{+2}, Mg^{+2} and K^+ as well as 260 and 280 nm absorbing materials was increased with increasing the concentration of anethole and Ant-eCsNe and reached maximum when fungal cells were treated with 2MIC (Fig. 3c and d; Fig. 4a). Ergosterol is a specific class of sterol found to be associated with fungal plasma membrane responsible for maintaining the fluidity and integrity of the cells. The lipophilic nature of anethole and its subcellular sizes after nanoencapsulation enabled them to interfere with the fungal plasma membrane causing disruption of ergosterol, resulting change in membrane permeability, leading to leakage of vital cellular constituents including ions and 260 and 280 nm absorbing materials, which are essential for maintaining cellular and metabolic energy status of the cells. The ascribed mechanism of chitosan action against fungi due to fungal cell membrane permeabilization and penetration has been also described by Romanazzi et al. (2017). In a previous work, Kelly et al. (1995) studied the antifungal mode of action of synthetic group of antifungal drugs and reported that the inhibition of fungal growth might be attributed to alteration in sterol metabolism. Some other studies have shown that the EOs and their bioactive compounds, which were claimed as food preservative, can also inhibit fungal growth by disrupting membrane ergosterol biosynthesis (Dwivedy et al. 2018; Upadhyay et al. 2018). Hence, the results of our study justified that the antifungal activity of anethole and Ant-eCsNe against AF-LHP-VS8 could be due, at least in part, to its ability to interfere with the integrity of the membrane by disrupting ergosterol, which can be used as a marker for the development of anethole and other active compound-based nanoformulations for practical use in food industries.

Table 3 Fungitoxic spectrum of anethole and Ant-eCsNe at MIC concentration

Moulds tested	Anethole	Ant-eCsNe
Aspregillus fumigatus	82.0 ± 4.7[b]	100 ± 0.0[a]
Aspergillus niger	100 ± 0.0[c]	100 ± 0.0[a]
Aspergillus luchuensis	100 ± 0.0[c]	100 ± 0.0[a]
Aspergillus repens	79.6 ± 1.2[a]	100 ± 0.0[a]
Penicillium italicum	87.9 ± 2.2[b]	100 ± 0.0[a]
Penicillium chrysogenum	100 ± 0.0[c]	100 ± 0.0[a]
Fusarium oxysporum	100 ± 0.0[c]	100 ± 0.0[a]
Alternaria alternata	100 ± 0.0[c]	100 ± 0.0[a]
Cladosporium cladosporioides	100 ± 0.0[c]	100 ± 0.0[a]

Values are presented as mean ± SE ($n = 3$)

[a–c] Significant differences at $p < 0.05$ level according to ANOVA (Tukey's B) multiple comparisons test

Antiaflatoxigenic Mechanism of Action of Anethole and Ant-eCsNe

The possible antiaflatoxigenic mechanism of action of anethole and Ant-eCsNe has been elucidated by measuring the level of methylglyoxal (MG) in AF-LHP-VS8 cells because of their direct involvement in enhancing the aflatoxin biosynthesis in *A. flavus* by speeding up the regulation of *afl*R gene (Chen et al. 2004). Both anethole and Ant-eCsNe caused concentration-dependent inhibition of MG with the value of 718.59–144.33 and 612.08–12.89 μM/g FW at 0.2–1.2 and 0.2–0.8 μL/mL concentrations, respectively (Fig. 4b). In contrast to anethole, Ant-eCsNe showed better efficacy in inhibiting MG. This result was comparable with those obtained by Upadhyay et al. (2018) and Singh et al. (2019), who suggested that the inhibition of MG might be the possible mechanism underlying aflatoxin suppression. Thus, based on our finding, we hypothesized that anethole and Ant-eCsNe may potentially inhibit AFB_1 production by downregulating the level of MG in cells. The finding appears to be the key that sheds light on important mechanism involved in AFB_1 inhibition and may be employed for the development of aflatoxin-resistant crop varieties through sustainable green

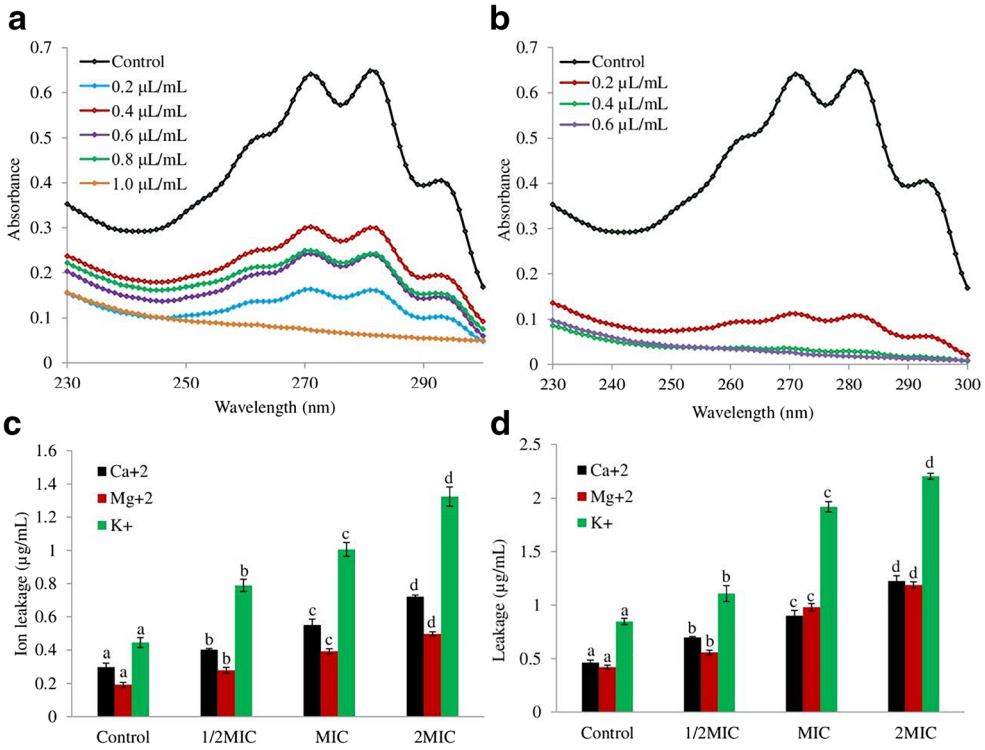

Fig. 3 **a** and **b** Effect of different concentrations of anethole and Ant-eCsNe on ergosterol and **c** and **d** cellular ions efflux

transgenic strategies; however, further study is needed to examine Ant-eCsNe activity over the fungal biochemical and molecular processes related to AFB_1 inhibition.

In Vivo Antifungal and Antiaflatoxigenic Evaluation of Anethole and Ant-eCsNe

As we can see from Fig. 5 a1–6, anethole showed remarkable antifungal activity and inhibited the visual growth of test fungus at 2MIC concentration, while Ant-eCsNe even at lower concentration (MIC) completely inhibited the fungal growth supporting the above finding of our results observed during in vitro evaluation of antifungal activity. The HPLC results (Fig. 5 b1–6) revealed that the level of AFB_1 in control samples ranged 2.75–3.68 µg/Kg, which was decreased to 0.42 and 0.07 µg/Kg in anethole-treated samples at MIC and 2MIC concentration, respectively (lesser than the limit set for AFB_1 in food samples by European Commission (2010), and could not be detected in any of the Ant-eCsNe-treated samples. The inhibition of AFB_1 may be due to inhibited biosynthesis of MG, i.e. reported to be an important metabolic substrate enhancing the level of aflatoxin in *A. flavus* justifying the antiaflatoxigenic mechanism of action as has been observed during in vitro investigation. The antifungal and antiaflatoxigenic potential of encapsulated anethole was found superior over most prevalently used organic acid preservatives, viz., benzoic acid, propionic acid, formic acid, acetic acid and sorbic acid (Prakash et al. 2012). Further, it should be noted that the lyophilization step of Ant-eCsNe lasted for 3 days;

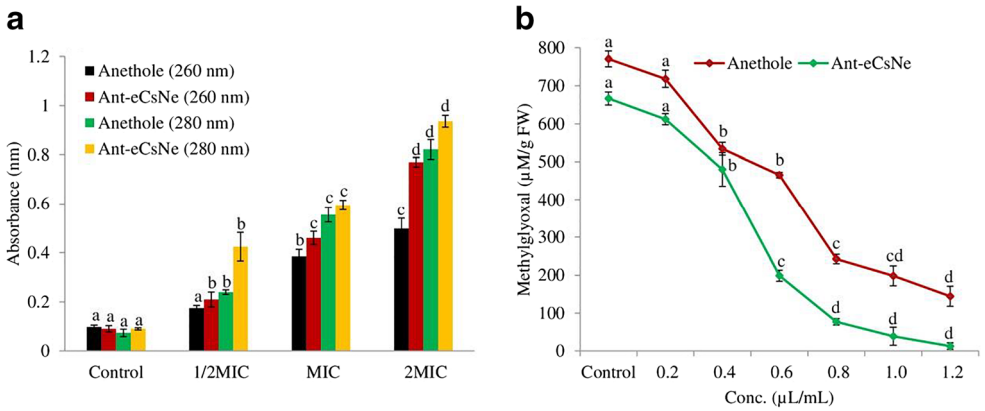

Fig. 4 Effect of different concentrations of anethole and Ant-eCsNe on (**a**) 260 and 280 nm absorbing materials efflux and (**b**) cellular methylglyoxal (MG) biosynthesis

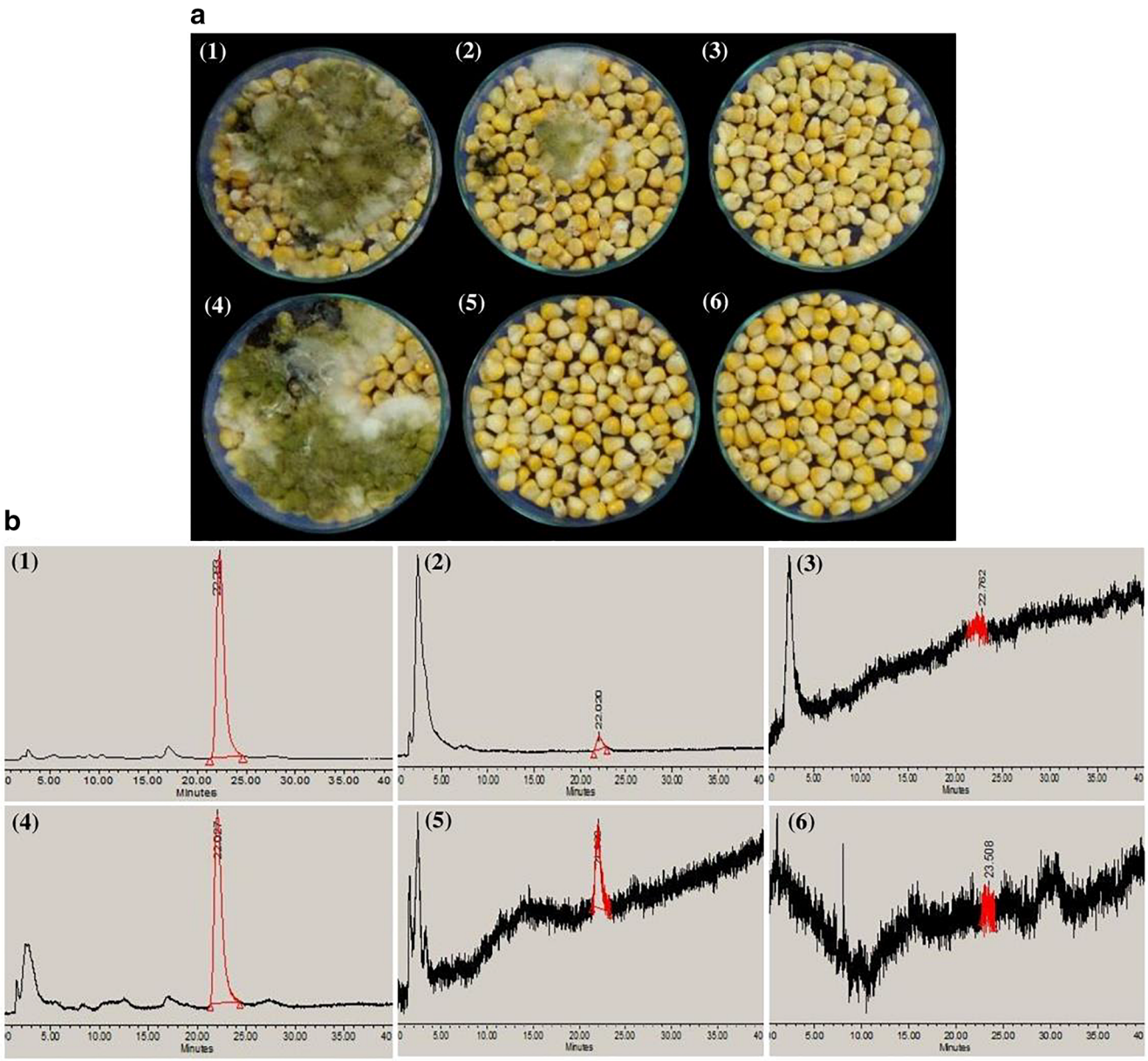

Fig. 5 In vivo antifungal and antiaflatoxigenic efficacy of anethole and Ant-eCsNe against AF-LHP-VS8 on maize samples; (**a1–3**) representative images of maize samples treated with 0, 1.2 μL/mL (MIC) and 2.4 μL/mL (2MIC) concentration of anethole; (**a4–6**) maize samples treated with 0, 0.8 μL/mL (MIC) and 1.6 μL/mL (2MIC) concentration of Ant-eCsNe; and (**b1–6**) HPLC chromatograms of maize samples treated with anethole and Ant-eCsNe at their respective (0, MIC and 2MIC) antifungal concentrations

hence, nanoemulsion became much stable during this step that possibly increased the functional performance of Ant-eCsNe for application in food industries. By virtue of its promising potential to inhibit growth and AFB_1 production, Ant-eCsNe can be recommended as novel antifungal preservative over un-encapsulated anethole and other synthetic preservatives in controlling deterioration of maize and other food commodities from fungal and AFB_1 contamination. Based on in vivo results, it is clear that the nanoencapsulation of anethole into chitosan nanoemulsion could provide a new horizon for maximizing their preservative potential in food industry. Most importantly, since a particular EO or its single compound may not be equally effective in protecting all kinds of food commodities because of considerable differences in nutritional composition, water activity, region of production and prevailing environmental conditions, therefore, this work was undertaken. However, further pilot-scale experiments are needed in order to ratify the efficacy of Ant-eCsNe in more realistic environment such as in storage chambers.

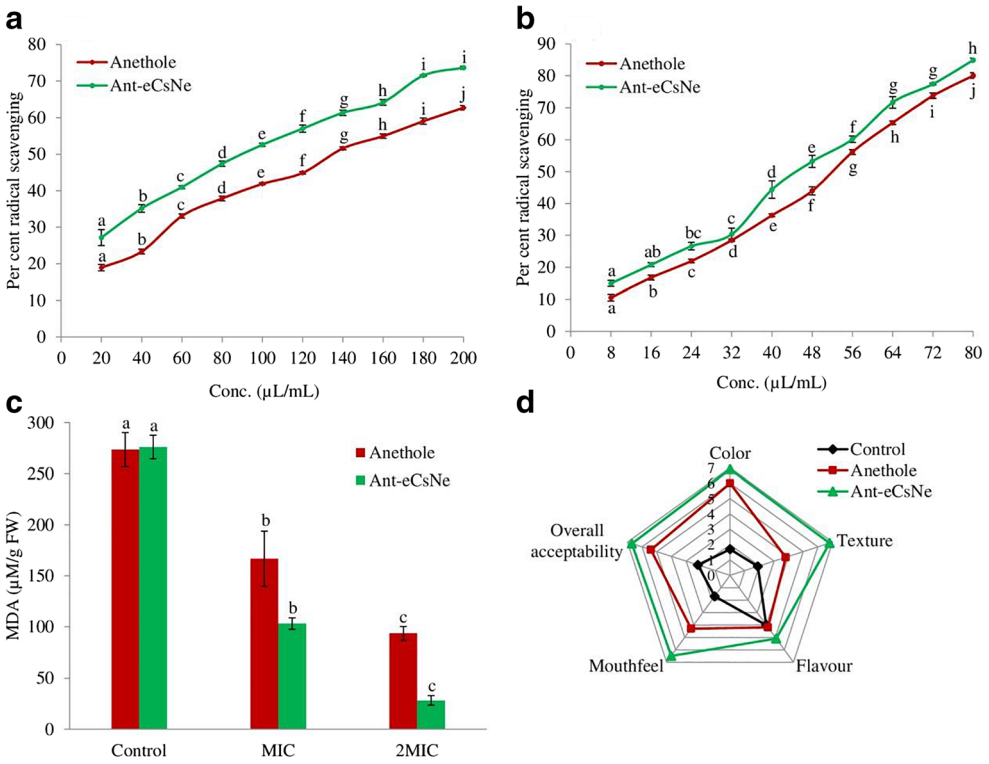

Fig. 6 **a** and **b** DPPH and ABTS radical scavenging activities of anethole and Ant-eCsNe. **c** Effect of anethole and Ant-eCsNe on lipid peroxidation of stored maize samples. **d** Hedonic scale plot showing the differences in sensory attributes of anethole and Ant-eCsNe-treated maize samples

Antioxidant Activity Determination of Anethole and Ant-eCsNe

The antioxidant activity of anethole and Ant-eCsNe was evaluated using the DPPH and ABTS assays, and the results are shown in Fig. 6a and b. Results evidenced that anethole exhibited concentration-dependent DPPH and ABTS radical scavenging activity with IC_{50} value 135.46 and 89.36 µL/mL, respectively. However, Ant-eCsNe showed better antioxidant activity with IC_{50} value 52.04 and 45.05 µL/mL against DPPH and ABTS radicals, respectively. The greater antioxidant activity of Ant-eCsNe than that of un-encapsulated anethole might be attributed to plenty of amino and hydroxyl moiety present on chitosan surface, which interacts and donates protons to free radicals generated in the medium (Ruiz-Navajas et al. 2013). Also, it is noteworthy that the low molecular weight of chitosan with high degree of deacetylation may also have profound impact on enhancing the antioxidant activity (Park et al. 2004). Currently, many synthetic antioxidants such as butylated hydroxyanisole, butylated hydroxytoluene, tertiary butylhydroquinone and propyl gallate are available and widely used in different food systems to lengthen their shelf-life; however, their negative concern regarding toxicity and consumer's demand for natural antioxidants has resulted in a growing trend for the utilization of natural antioxidants (Domínguez et al. 2018; Chaudhari et al. 2019). In this regard, the encapsulated anethole with enhanced free radical scavenging activities could provide an exciting potential for the future applications, and food industries may consider the employment of this novel nanoemulsion as a natural substitute of synthetic antioxidants for direct application in food system.

Effect of Anethole and Ant-CsNe on Inhibition of Lipid Oxidation

Results of lipid oxidation inhibition in food system (maize samples) by anethole and Ant-eCsNe are presented in Fig. 6c. It can be observed that anethole significantly inhibited the amount of MDA from 166.80 ± 27.12 µg MDA/g FW at MIC to 103.20 ± 24.90 µg MDA/g FW at 2MIC. On the other hand, Ant-eCsNe at MIC and 2MIC concentration presented higher lipid oxidation inhibition activity with lower MDA content, i.e. 75.30 ± 5.72 and 24.90 ± 4.65 µg MDA/g FW, respectively. This may occur because free radical scavengers present in anethole together with chitosan can terminate the propagation steps induced by free radical intermediates either by reacting or by preventing breakdown of nonreacting free radicals to reacting radicals (Talón et al. 2017). The results of lipid oxidation inhibition potential of Ant-eCsNe in the present study are in good agreement with the results previously reported in the literature (Djenane et al. 2012; Ghaderi-Ghahfarokhi et al. 2016) focussing on the preservative effects of *Lavandula* and *Mentha* EO and encapsulated *Thymus* EO, respectively, on suppressing the lipid oxidation of minced meat and beef burger during refrigerated storage. The effectiveness of the Ant-eCsNe against maize lipid oxidation confirms the result of in vitro assessment of antioxidant activity that demonstrated its strong ability of scavenging free radicals

generated by lipid oxidation. In the present assay, TBA reacts with the toxic MDA produced during lipid oxidation reaction of maize samples to form a pink colour adduct that was calorimetrically recorded at 532 nm. TBA assay quantifying the MDA in the samples, being the typical indicator of lipid rancidity, provides useful information regarding lipid oxidation of food samples (Xu et al. 2009). Hence, it can be inferred that Ant-eCsNe had superior potential for restricting the process of lipid oxidation compared with synthetic preservatives, thereby offering great opportunity to be applied in food industries as an accessible source of natural shelf-life enhancer of stored maize samples.

Sensory Analysis: Effect on Organoleptic Attributes

Because the major objective of this study is to recommend the nanoencapsulated anethole for use in preservation of maize and other stored food items, it is compulsory to ensure whether the nanoencapsulation really affects consumer's willingness. For this, a sensory analysis was conducted on maize samples treated with anethole and Ant-eCsNe as described in materials and methods section. For both food samples (either treated with anethole or Ant-eCsNe), there was a considerable variability in perception of sensory attributes among assessors as can be observed from the results (Fig. 6d). Concerning anethole-treated maize samples, there was a low score for texture, aroma and mouth feel, representing that it had significant negative impact on sensory characteristics but lesser than the control samples (scored lowest for almost all the tested parameters). However, when evaluation was made for Ant-eCsNe, there were good scores for all the parameters, viz. colour, texture, flavour, mouth feel and the overall acceptability. The result showed that Ant-eCsNe had no adverse effects on perception of sensory attributes of maize samples; hence, it can be a preferred choice to be used as preservative for increasing the shelf-life of stored maize samples. The overall sensory acceptability of anethole-enriched chitosan was found better in comparison with other chemical preservatives such as sodium benzoate and potassium metabisulphite, supporting its utilization in food industries (Durrani et al. 2010). Moreover, after encapsulation into chitosan nanomatrix, the volatility of anethole was retained, thereby significantly improving the sensory perception of the treated maize samples.

Conclusion

The chitosan nanoemulsion containing anethole (Ant-eCsNe) exhibited enhanced antifungal, antiaflatoxigenic and antioxidant efficacy against fungal infestation, AFB_1 secretion and lipid oxidation. Ant-eCsNe inhibited methylglyoxal biosynthesis, signifying novel antiaflatoxigenic mechanism of action and highlights its importance for the introduction of aflatoxin-resistant crop varieties through green transgenic approach. The findings of the present study recommend Ant-eCsNe as a novel green preservative for stored maize samples in view of its efficacy to suppress *A. flavus* growth and AFB_1 biosynthesis as well as lipid oxidation in maize samples at lower concentrations during in vivo investigations and acceptable sensory performance.

Acknowledgements Authors are thankful to the Head, CAS, DST-PURSE, Banaras Hindu University for providing laboratory facilities and Indian Institute of Technology, Banaras Hindu University for FTIR, SEM and XRD analysis.

Funding Information Anand Kumar Chaudhari is thankful to Council of Scientific and Industrial Research (CSIR) [09/013(0678)/2017-EMR-I], New Delhi, India for providing senior research fellowship.

Compliance with Ethical Standards

Conflict of Interest The authors declare that they have no conflict of interest.

References

Ahmadi, Z., Saber, M., Akbari, A., & Mahdavinia, G. R. (2018). Encapsulation of *Satureja hortensis* L.(Lamiaceae) in chitosan/TPP nanoparticles with enhanced acaricide activity against *Tetranychus urticae* Koch (Acari: Tetranychidae). *Ecotoxicology and Environmental Safety, 161*, 111–119.

Amiri, A., Mousakhani-Ganjeh, A., Amiri, Z., Guo, Y. G., Singh, A. P., & Kenari, R. E. (2020). Fabrication of cumin loaded-chitosan particles: Characterized by molecular, morphological, thermal, antioxidant and anticancer properties as well as its utilization in food system. *Food Chemistry, 310*, 125821.

Anitha, A., Deepagan, V. G., Rani, V. D., Menon, D., Nair, S. V., & Jayakumar, R. (2011). Preparation, characterization, in vitro drug release and biological studies of curcumin loaded dextran sulphate–chitosan nanoparticles. *Carbohydrate Polymers, 84*(3), 1158–1164.

Avanço, G. B., Ferreira, F. D., Bomfim, N. S., Peralta, R. M., Brugnari, T., Mallmann, C. A., & Machinski Jr., M. (2017). *Curcuma longa* L. essential oil composition, antioxidant effect, and effect on *Fusarium verticillioides* and fumonisin production. *Food Control, 73*, 806–813.

Aydogdu, A., Sumnu, G., & Sahin, S. (2019). Fabrication of gallic acid loaded hydroxypropyl methylcellulose nanofibers by electrospinning technique as active packaging material. *Carbohydrate Polymers, 208*, 241–250.

Battilani, P., Toscano, P., Van der Fels-Klerx, H. J., Moretti, A., Leggieri, M. C., Brera, C., & Robinson, T. (2016). Aflatoxin B1 contamination in maize in Europe increases due to climate change. *Scientific Reports, 6*(1), 24328.

Beyki, M., Zhaveh, S., Khalili, S. T., Rahmani-Cherati, T., Abollahi, A., Bayat, M., & Mohsenifar, A. (2014). Encapsulation of *Mentha piperita* essential oils in chitosan–cinnamic acid nanogel with enhanced antimicrobial activity against *Aspergillus flavus*. *Industrial Crops and Products, 54*, 310–319.

Bugnicourt, L., & Ladavière, C. (2016). Interests of chitosan nanoparticles ionically cross-linked with tripolyphosphate for biomedical applications. *Progress in Polymer Science, 60*, 1–17.

Carocho, M., Barreiro, M. F., Morales, P., & Ferreira, I. C. (2014). Adding molecules to food, pros and cons: A review on synthetic and natural food additives. *Comprehensive Reviews in Food Science and Food Safety, 13*(4), 377–399.

Castro, M. F. P. M. D., Bragagnolo, N., & Valentini, S. R. D. T. (2002). The relationship between fungi growth and aflatoxin production with ergosterol content of corn grains. *Brazilian Journal of Microbiology, 33*(1), 22–26.

Chaudhari, A. K., Dwivedy, A. K., Singh, V. K., Das, S., Singh, A., & Dubey, N. K. (2019). Essential oils and their bioactive compounds as green preservatives against fungal and mycotoxin contamination of food commodities with special reference to their nanoencapsulation. *Environmental Science and Pollution Research, 26*(25), 25414–25431.

Chaudhari, A. K., Singh, V. K., Dwivedy, A. K., Das, S., Upadhyay, N., Singh, A., & Dubey, N. K. (2018). Chemically characterised *Pimenta dioica* (L.) Merr. essential oil as a novel plant based antimicrobial against fungal and aflatoxin B1 contamination of stored maize and its possible mode of action. *Natural Product Research, 34*, 745–749.

Chen, Z. Y., Brown, R. L., Damann, K. E., & Cleveland, T. E. (2004). Identification of a maize kernel stress-related protein and its effect on aflatoxin accumulation. *Phytopathology, 94*(9), 938–945.

Commission Regulation (EU) No 165/2010, Amending Regulation (EC) No 1881/2006 setting maximum levels for certain contaminants in foodstuffs as regards aflatoxins. 2010. Accessed date: 26 February 2010.

Contigiani, E. V., Jaramillo-Sánchez, G., Castro, M. A., Gómez, P. L., & Alzamora, S. M. (2018). Postharvest quality of strawberry fruit (Fragaria x Ananassa Duch cv. Albion) as affected by ozone washing: Fungal spoilage, mechanical properties, and structure. *Food and Bioprocess Technology, 11*(9), 1639–1650.

Das, S., Singh, V. K., Dwivedy, A. K., Chaudhari, A. K., Upadhyay, N., Singh, P., & Dubey, N. K. (2019). Encapsulation in chitosan-based nanomatrix as an efficient green technology to boost the antimicrobial, antioxidant and in situ efficacy of *Coriandrum sativum* essential oil. *International Journal of Biological Macromolecules, 133*, 294–305.

Dash, M., Chiellini, F., Ottenbrite, R. M., & Chiellini, E. (2011). Chitosan—A versatile semi-synthetic polymer in biomedical applications. *Progress in Polymer Science, 36*(8), 981–1014.

Djenane, D., Aïder, M., Yangüela, J., Idir, L., Gómez, D., & Roncalés, P. (2012). Antioxidant and antibacterial effects of Lavandula and Mentha essential oils in minced beef inoculated with E. coli O157: H7 and *S. aureus* during storage at abuse refrigeration temperature. *Meat Science, 92*(4), 667–674.

Domínguez, R., Barba, F. J., Gómez, B., Putnik, P., Kovačević, D. B., Pateiro, M., & Lorenzo, J. M. (2018). Active packaging films with natural antioxidants to be used in meat industry: A review. *Food Research International, 113*, 93–101.

Donsì, F., Annunziata, M., Sessa, M., & Ferrari, G. (2011). Nanoencapsulation of essential oils to enhance their antimicrobial activity in foods. *LWT-Food Science and Technology, 44*(9), 1908–1914.

Durrani, Y., Ayub, M., Muhammad, A., & Ali, A. (2010). Physicochemical response of apple pulp to chemical preservatives and antioxidant during storage. *International Journal of Food Safety, 12*, 20–28.

Dwivedy, A. K., Singh, V. K., Prakash, B., & Dubey, N. K. (2018). Nanoencapsulated *Illicium verum* Hook. f. essential oil as an effective novel plant-based preservative against aflatoxin B1 production and free radical generation. *Food and Chemical Toxicology, 111*, 102–113.

Ezhilarasi, P. N., Karthik, P., Chhanwal, N., & Anandharamakrishnan, C. (2013). Nanoencapsulation techniques for food bioactive components: A review. *Food and Bioprocess Technology, 6*(3), 628–647.

Fan, X. (2002). Measurement of malonaldehyde in apple juice using GC–MS and a comparison to the thiobarbituric acid assay. *Food Chemistry, 77*(3), 353–359.

Gahruie, H. H., Ziaee, E., Eskandari, M. H., & Hosseini, S. M. H. (2017). Characterization of basil seed gum-based edible films incorporated with *Zataria multiflora* essential oil nanoemulsion. *Carbohydrate Polymers, 166*, 93–103.

Ghaderi-Ghahfarokhi, M., Barzegar, M., Sahari, M. A., & Azizi, M. H. (2016). Nanoencapsulation approach to improve antimicrobial and antioxidant activity of thyme essential oil in beef burgers during refrigerated storage. *Food and Bioprocess Technology, 9*(7), 1187–1201.

Gómez, J. V., Tarazona, A., Mateo-Castro, R., Gimeno-Adelantado, J. V., Jiménez, M., & Mateo, E. M. (2018). Selected plant essential oils and their main active components, a promising approach to inhibit aflatoxigenic fungi and aflatoxin production in food. *Food Additives & Contaminants: Part A, 35*(8), 1581–1595.

Guo, M., Yadav, M. P., & Jin, T. Z. (2017). Antimicrobial edible coatings and films from micro-emulsions and their food applications. *International Journal of Food Microbiology, 263*, 9–16.

Hasheminejad, N., Khodaiyan, F., & Safari, M. (2019). Improving the antifungal activity of clove essential oil encapsulated by chitosan nanoparticles. *Food Chemistry, 275*, 113–122.

Hosseini, S. F., Zandi, M., Rezaei, M., & Farahmandghavi, F. (2013). Two-step method for encapsulation of oregano essential oil in chitosan nanoparticles: Preparation, characterization and in vitro release study. *Carbohydrate Polymers, 95*(1), 50–56.

Jayakumar, R., Reis, R. L., & Mano, J. F. (2007). Synthesis and characterization of pH-sensitive thiol-containing chitosan beads for controlled drug delivery applications. *Drug Delivery, 14*(1), 9–17.

Juárez-Morales, L. A., Hernandez-Cocoletzi, H., Chigo-Anota, E., Aguila-Almanza, E., & Tenorio-Arvide, M. G. (2017). Chitosan-aflatoxins B1, M1 interaction: A computational approach. *Current Organic Chemistry, 21*(28), 2877–2883.

Keawchaoon, L., & Yoksan, R. (2011). Preparation, characterization and in vitro release study of carvacrol-loaded chitosan nanoparticles. *Colloids and Surfaces B: Biointerfaces, 84*(1), 163–171.

Kelly, S. L., Lamb, D. C., Corran, A. J., Baldwin, B. C., & Kelly, D. E. (1995). Mode of action and resistance to azole antifungals associated with the formation of 14α-methylergosta-8, 24 (28)-dien-3β, 6α-diol. *Biochemical and Biophysical Research Communications, 207*(3), 910–915.

Kfoury, M., Auezova, L., Greige-Gerges, H., Ruellan, S., & Fourmentin, S. (2014). Cyclodextrin, an efficient tool for trans-anethole encapsulation: Chromatographic, spectroscopic, thermal and structural studies. *Food Chemistry, 164*, 454–461.

Kos, J., Mastilović, J., Hajnal, E. J., & Šarić, B. (2013). Natural occurrence of aflatoxins in maize harvested in Serbia during 2009–2012. *Food Control, 34*(1), 31–34.

Ksouda, G., Sellimi, S., Merlier, F., Falcimaigne-Cordin, A., Thomasset, B., Nasri, M., & Hajji, M. (2019). Composition, antibacterial and antioxidant activities of *Pimpinella saxifraga* essential oil and application to cheese preservation as coating additive. *Food Chemistry, 288*, 47–56.

Kumar, A., Shukla, R., Singh, P., Prasad, C. S., & Dubey, N. K. (2008). Assessment of *Thymus vulgaris* L. essential oil as a safe botanical preservative against post harvest fungal infestation of food commodities. *Innovative Food Science & Emerging Technologies, 9*(4), 575–580.

Lim, C. T., Tan, E. P. S., & Ng, S. Y. (2008). Effects of crystalline morphology on the tensile properties of electrospun polymer nanofibers. *Applied Physics Letters, 92*(14), 141908.

Lin, L., Zhu, Y., Thangaraj, B., Abdel-Samie, M. A., & Cui, H. (2018). Improving the stability of thyme essential oil solid liposome by using β-cyclodextrin as a cryoprotectant. *Carbohydrate Polymers, 188*, 243–251.

López-Meneses, A. K., Plascencia-Jatomea, M., Lizardi-Mendoza, J., Fernández-Quiroz, D., Rodríguez-Félix, F., Mouriño-Pérez, R. R., & Cortez-Rocha, M. O. (2018). *Schinus molle* L. essential oil-loaded chitosan nanoparticles: Preparation, characterization, antifungal and anti-aflatoxigenic properties. *LWT-Food Science and Technology, 96*, 597–603.

Mahuku, G., Nzioki, H. S., Mutegi, C., Kanampiu, F., Narrod, C., & Makumbi, D. (2019). Pre-harvest management is a critical practice for minimizing aflatoxin contamination of maize. *Food Control, 96*, 219–226.

Medeiros, B. G. D. S., Souza, M. P., Pinheiro, A. C., Bourbon, A. I., Cerqueira, M. A., Vicente, A. A., & Carneiro-da-Cunha, M. G. (2014). Physical characterisation of an alginate/lysozyme nanolaminate coating and its evaluation on 'Coalho'cheese shelf life. *Food and Bioprocess Technology, 7*(4), 1088–1098.

Muxika, A., Etxabide, A., Uranga, J., Guerrero, P., & De La Caba, K. (2017). Chitosan as a bioactive polymer: Processing, properties and applications. *International Journal of Biological Macromolecules, 105*(Pt 2), 1358–1368.

Newberne, P., Smith, R. L., Doull, J., Goodman, J. I., Munro, I. C., Portoghese, P. S., & Lucas, C. D. (1999). The FEMA GRAS assessment of trans-anethole used as a flavouring substance. *Food and Chemical Toxicology, 37*(7), 789–811.

Nishimwe, K., Wanjuki, I., Karangwa, C., Darnell, R., & Harvey, J. (2017). An initial characterization of aflatoxin B1 contamination of maize sold in the principal retail markets of Kigali, Rwanda. *Food Control, 73*, 574–580.

Osorio-Madrazo, A., David, L., Trombotto, S., Lucas, J. M., Peniche-Covas, C., & Domard, A. (2010). Kinetics study of the solid-state acid hydrolysis of chitosan: Evolution of the crystallinity and macromolecular structure. *Biomacromolecules, 11*(5), 1376–1386.

Othman, N., Masarudin, M. J., Kuen, C. Y., Dasuan, N. A., Abdullah, L. C., Jamil, M., & Ain, S. N. (2018). Synthesis and optimization of chitosan nanoparticles loaded with l-ascorbic acid and thymoquinone. *Nanomaterials, 8*(11), 920.

Pabast, M., Shariatifar, N., Beikzadeh, S., & Jahed, G. (2018). Effects of chitosan coatings incorporating with free or nano-encapsulated Satureja plant essential oil on quality characteristics of lamb meat. *Food Control, 91*, 185–192.

Park, P. J., Je, J. Y., & Kim, S. K. (2004). Free radical scavenging activities of differently deacetylated chitosans using an ESR spectrometer. *Carbohydrate Polymers, 55*(1), 17–22.

Prakash, B., Kujur, A., Yadav, A., Kumar, A., Singh, P. P., & Dubey, N. K. (2018). Nanoencapsulation: An efficient technology to boost the antimicrobial potential of plant essential oils in food system. *Food Control, 89*, 1–11.

Prakash, B., Shukla, R., Singh, P., Kumar, A., Mishra, P. K., & Dubey, N. K. (2010). Efficacy of chemically characterized Piper betle L. essential oil against fungal and aflatoxin contamination of some edible commodities and its antioxidant activity. *International Journal of Food Microbiology, 142*(1-2), 114–119.

Prakash, B., Singh, P., Mishra, P. K., & Dubey, N. K. (2012). Safety assessment of *Zanthoxylum alatum* Roxb. essential oil, its antifungal, antiaflatoxin, antioxidant activity and efficacy as antimicrobial in preservation of *Piper nigrum* L. fruits. *International Journal of Food Microbiology, 153*(1-2), 183–191.

Rammanee, K., & Hongpattarakere, T. (2011). Effects of tropical citrus essential oils on growth, aflatoxin production, and ultrastructure alterations of *Aspergillus flavus* and *Aspergillus parasiticus*. *Food and Bioprocess Technology, 4*(6), 1050–1059.

Robledo, N., Vera, P., López, L., Yazdani-Pedram, M., Tapia, C., & Abugoch, L. (2018). Thymol nanoemulsions incorporated in quinoa protein/chitosan edible films; antifungal effect in cherry tomatoes. *Food Chemistry, 246*, 211–219.

Romanazzi, G., Feliziani, E., Baños, S. B., & Sivakumar, D. (2017). Shelf life extension of fresh fruit and vegetables by chitosan treatment. *Critical Reviews in Food Science and Nutrition, 57*(3), 579–601.

Ruiz-Navajas, Y., Viuda-Martos, M., Sendra, E., Perez-Alvarez, J. A., & Fernández-López, J. (2013). In vitro antibacterial and antioxidant properties of chitosan edible films incorporated with *Thymus moroderi* or *Thymus piperella* essential oils. *Food Control, 30*(2), 386–392.

Singh, V. K., Das, S., Dwivedy, A. K., Rathore, R., & Dubey, N. K. (2019). Assessment of chemically characterized nanoencapuslated *Ocimum sanctum* essential oil against aflatoxigenic fungi contaminating herbal raw materials and its novel mode of action as methyglyoxal inhibitor. *Postharvest Biology and Technology, 153*, 87–95.

Talón, E., Trifkovic, K. T., Nedovic, V. A., Bugarski, B. M., Vargas, M., Chiralt, A., & González-Martínez, C. (2017). Antioxidant edible films based on chitosan and starch containing polyphenols from thyme extracts. *Carbohydrate Polymers, 157*, 1153–1161.

Upadhyay, N., Singh, V. K., Dwivedy, A. K., Das, S., Chaudhari, A. K., & Dubey, N. K. (2018). *Cistus ladanifer* L. essential oil as a plant based preservative against molds infesting oil seeds, aflatoxin B1 secretion, oxidative deterioration and methylglyoxal biosynthesis. *LWT-Food Science and Technology, 92*, 395–403.

Wei, L., Li, Q., Chen, Y., Zhang, J., Mi, Y., Dong, F., & Guo, Z. (2019). Enhanced antioxidant and antifungal activity of chitosan derivatives bearing 6-O-imidazole-based quaternary ammonium salts. *Carbohydrate Polymers, 206*, 493–503.

Xu, W. T., Peng, X. L., Luo, Y. B., Wang, J. A., Guo, X., & Huang, K. L. (2009). Physiological and biochemical responses of grapefruit seed extract dip on 'Redglobe'grape. *LWT-Food Science and Technology, 42*(2), 471–476.

Ye, Y., Zhu, M., Miao, K., Li, X., Li, D., & Mu, C. (2017). Development of antimicrobial gelatin-based edible films by incorporation of trans-anethole/β-cyclodextrin inclusion complex. *Food and Bioprocess Technology, 10*(10), 1844–1853.

Yoksan, R., Jirawutthiwongchai, J., & Arpo, K. (2010). Encapsulation of ascorbyl palmitate in chitosan nanoparticles by oil-in-water emulsion and ionic gelation processes. *Colloids and Surfaces B: Biointerfaces, 76*(1), 292–297.